From:	Yang, Nelson
Sent:	Tuesday, October 07, 2003 3:39 PM
To:	STIC-ILL
Subject:	ILL_Order

ILL Ordering Information:

Art Unit or Location: 1641

Telephone Number: 703-305-4508

Application Number or Other Order Identifier: 09970434

Below is the suggested reference ordering information that STIC needs to locate each reference. You may choose to cut and paste a citation containing this information, rather than filling in the details manually.

Author (if known): **Klauson A, Metsaveer J.**

Article Title: **Sound scattering by a cylindrical shell reinforced by lengthwise ribs and walls**

Journal or Book Title: J Acoust Soc Am. .

Pages if a Journal: 1834-43

Volume and Issue if a Journal: 91(4 Pt 1):

Year of Publication: 1992 Apr;

Sound scattering by a cylindrical shell reinforced by lengthwise ribs and walls

Aleksander Klauson and Jaan Metsaveer
Department of Structural Mechanics, Tallinn Technical University, Akadeemia tee, 1, 200108 Tallinn, Estonia

An analytical solution is derived for the acoustic response of submerged thin-walled ring cylindrical shell containing lengthwise stiffening members: internal stringers and walls. On the basis of the analysis of the acoustic pressure versus time diagrams the stiffener-borne wave-generation mechanisms are traced. Shown is that the shell/stiffener junctions act as additional entry and exit points of circumferential waves circulating in the shell and the fluid. The stiffening members cause transformations of circumferential waves from one propagation type to another.

PACS numbers: 43.20.Fn

INTRODUCTION

A growing interest in surface wave phenomena in submerged vibrating structures leads to the problem of the sound scattering and radiation by elastic bodies containing structural nonuniformities. The problem can be treated analytically in the case of scatterers having a surface that coincides with a coordinate surface in a separable coordinate system and nonuniformities lying along coordinate lines, for example, a reinforcement, which may be attached regularly or irregularly to the main body of the structure.

Acoustic radiation by surface-impedance nonuniformities has been investigated by Maidanik,[1] and Maidanik and Crighton.[2] Shown is the role of the impedance nonuniformities as wave number convertors, changing acoustic field subsonic components into supersonic ones, which results in the growth of radiation efficiency. The sound fields generated by fluid-loaded stiffened plates were investigated by Konovaljuk and Krasilnikov[3] in the case of single internal rib, and by Belinskii[4] in the case of an external rib being in contact with a surrounding fluid.

The scattering problem for an infinitely long cylindrical shell reinforced by evenly spaced rigid septa has been formulated by Junger.[5] Forced vibration of a fluid-loaded cylindrical shell reinforced by elastic ring supports was discussed by Bernblit[6] and the sound radiation by a cylindrical shell having doubly periodic ring supports by Burroughs.[7] Shown is the presence of two radiation mechanisms: radiation by lower wave numbers in the structural near field of the driving force and scattering by ring supports with conversion of higher wave numbers into lower ones. Evseev[8] has solved the sound radiation problem in the case of a cylindrical shell with a periodic set of equidistant lengthwise supports.

In our previous paper[9] the problem of the sound scattering by a cylindrical shell with an arbitrary set of lengthwise supports (stringers) has been solved analytically. The wave scattering mechanism has been traced in the model of a shell with a single stringer, which does not restrict generalizations for the more complicated reinforcement structure. An additional wave-formation mechanism is shown to consist of penetrating circumferential bending propagation type waves through the shell/stiffener junction line, which takes place in a relatively wider frequency range than in the case of unstiffened shell. However, wave processes in the stiffening members have not been considered ("rigid" stiffeners). The present paper is a more detailed investigation of wave generation mechanisms in lengthwise stiffening members like stringers and internal walls.

I. THE PROBLEM

Let a thin-walled elastic ring cylindrical shell of centroidal radius R and thickness h be immersed in an unbounded ideal fluid medium with a density ρ and sound velocity c. The shell material is isotropic, has a density ρ_1, and is characterized by elastic constants E, v. There is a vacuum inside the shell. A shell is supported from inside by an arbitrary set of S internal stringers and walls, not being in contact with each other [Fig. 1(a)]. The radial dimension of a rib is l, and its thickness is h_s. Stiffener material parameters are ρ_s, E_s, and v_s. The shell is insonified by a plane acoustic pulse p_i of normal incidence. Required is the determination of the outer sound pressure field p generated by an incident wave.

To describe the given two-dimensional (2-D) problem, the polar coordinates (r,θ) are attached to the shell [Fig. 1(b)].

II. BASIC EQUATIONS

Sound pressure p in fluid obeys the wave equation

$$\left(\nabla^2 - \frac{1}{c^2}\frac{\partial^2}{\partial t^2}\right)p = 0, \tag{1}$$

subject to a contact boundary condition at the shell surface

$$\frac{\partial}{\partial r}(p_i + p)|_{r=R} = -\rho\frac{\partial^2}{\partial t^2}u_3, \tag{2}$$

where u_3 is the shell normal displacement. Initial conditions are taken to be equal to zero. The Timoshenko–Mindlin[10] theory of plates and shells, which takes into account shear deformation and rotational inertia, is used to describe the
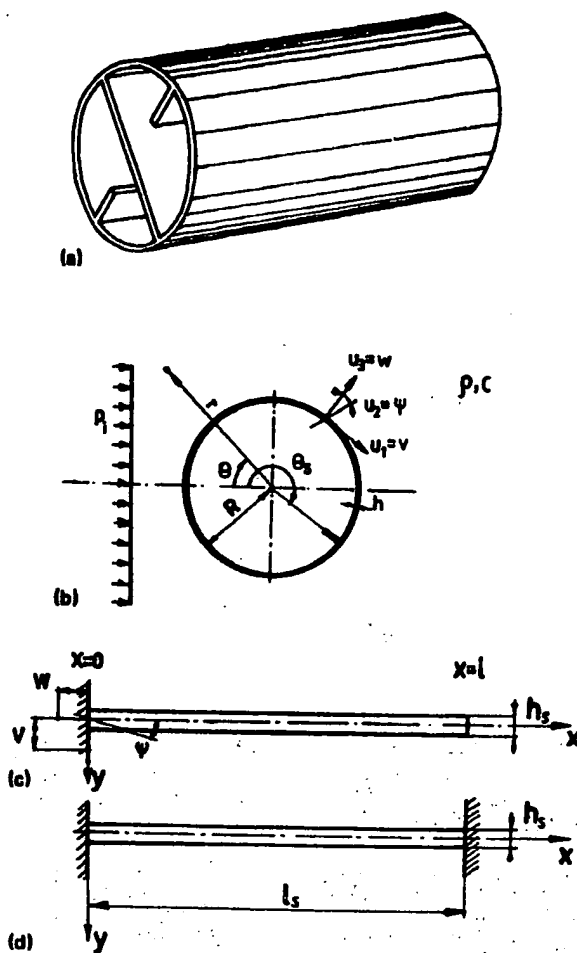
FIG. 1. Geometry of the problem. (a), (b) Reinforced shell; (c) stringer; (d) internal wall.

motions of the shell and the stiffening members. If the thicknesses of the stiffening members and the shell are of the same smallness order one can assume them to be joined along lines.

The Fourier transform is taken to solve the given time-dependent problem.

Hence all parameters of the structure are normalized with respect to the radius R of the centroidal surface of the shell and fluid parameters ρ and c so that the transformed shell theory equations aquire the form

$$L_{ij}u_j = \delta_{i3}q_r|_{r=R} + \sum_{s=1}^{S} f_{ijs}u_j\delta(\theta - \theta_s), \quad i,j = 1,2,3,$$

$$q_r = \xi^{-1}\rho^{-1}c^{-2}(p_i + p), \tag{3}$$

where differential operators are

$$L_{11} = (1 + a^2)\left(\frac{\partial^2}{\partial\theta^2} - \kappa^2\right) + \beta^{-2}\omega^2,$$

$$L_{12} = a^2\left(-\frac{\partial^2}{\partial\theta^2} + \kappa^2 + \beta^{-2}\omega^2\right) + \kappa^2,$$

$$L_{13} = (1 + a^2)(1 + \kappa^2)\frac{\partial}{\partial\theta},$$

$$L_{23} = -[(1 + a^2)\kappa^2 + a^2]\frac{\partial}{\partial\theta},$$

$$L_{33} = (1 + a^2)\left(\kappa^2\frac{\partial^2}{\partial\theta^2} - 1\right) + \beta^{-2}\omega^2,$$

$$L_{21} = L_{12}, \quad L_{31} = -L_{13}, \quad L_{32} = -L_{23},$$

$$a = \frac{h}{(R\sqrt{12})}, \quad \kappa = \frac{c_{20}}{c_{10}}, \quad \beta = \frac{c_{10}}{c},$$

$$c_{10}^2 = E/[\rho_1(1 - \nu^2)], \quad c_{20}^2 = Ek_t/[2\rho_1(1 + \nu)],$$

$$\xi = \beta^2 h\rho_1/(R\rho), \quad k_t = \pi^2/12,$$

c_{10} and c_{20} are wave front velocities, and k_t is the shear coefficient. Displacements $u_1 = v/R$ and $u_3 = w/R$ are dimensionless with respect to the radius R tangential, and normal displacements, respectively, $u_2 = \psi$ is angular in the radial plane displacement [Fig. 1(b)], ω is the dimensionless frequency ($\omega = \Omega R/c = kR$, where Ω is the angular frequency of the perturbation and k is the wavelength), δ_{in} is Kronecker's symbol; and f_{ijs} denotes the stiffener's reaction to the unit displacement of the shell.

In accordance with Timoshenko–Mindlin theory, an elastic stringer, attached to the point with coordinate $\theta = \theta_s$ [Fig. 1(c)], has reactions[11]

$$f_{11s} = Q(0)|_{v(0)=1}$$

$$= -e_s l_s^{-3}k_3k_4(k_1k_3 + k_2k_4)$$

$$\times(k_2^2k_4 \, \text{ch} \, k_2 \sin k_1 + k_1^2k_3 \, \text{sh} \, k_2 \cos k_1)f_1^{-1},$$

$$f_{12s} = Q(0)|_{\psi(0)=1}$$

$$= e_s l_s^{-2}k_3k_4[k_1k_2(k_1k_3 - k_2k_4)$$

$$\times(\text{ch} \, k_2 \cos k_1 - 1)$$

$$+ (k_1^3k_3 + k_2^3k_4) \, \text{sh} \, k_2 \sin k_1]f_1^{-1},$$

$$f_{21s} = M(0)|_{v(0)=1} = f_{12s}, \quad f_{13s} = f_{23s} = f_{31s} = f_{32s},$$

$$f_{22s} = M(0)|_{\psi(0)=1}$$

$$= -e_s l_s^{-1}(k_1k_3 + k_2k_4)(k_1^2k_3 \, \text{ch} \, k_2 \sin k_1$$

$$- k_2^2k_4 \, \text{sh} \, k_2 \cos k_1)f_1^{-1},$$

$$f_{33s} = N(0)|_{w(0)=1} = -E_sA_sl_s^{-1}h^{-1}k_5 \tan k_5,$$

$$f_1(k_1,k_2) = 2k_1k_2k_3k_4 + k_3k_4(k_2^2 - k_1^2)$$

$$\times \text{sh} \, k_2 \sin k_1 + (k_1^2k_3^2 + k_2^2k_4^2)$$

$$\times \text{ch} \, k_2 \cos k_1,$$

and an elastic internal wall, attached at the points with coordinates θ_s and $\theta_s + \pi$ [Fig. 1(d)], has reactions[11]

$$f_{11s}^{(0)} = Q(0)|_{v(0)=1}$$

$$= e_s l_s^{-3}k_3k_4(k_1k_3 + k_2k_4)$$

$$\times(k_3 \, \text{ch} \, k_2 \sin k_1 + k_4 \, \text{sh} \, k_2 \cos k_1)f_2^{-1},$$

$$f_{11s}^{(l)} = Q(l)|_{v(l)=1}$$

$$= e_s l_s^{-3}k_3k_4(k_1k_3 + k_2k_4)$$

$$\times(k_4 \, \text{sh} \, k_2 + k_3 \sin k_1)f_2^{-1},$$

$$f_{12s}^{(0)} = Q(0)|_{\psi(0)=1}$$
$$= -e_s l_s^{-2} k_3 k_4 [(k_2 k_4 - k_1 k_3)(\operatorname{ch} k_2 \cos k_1 - 1)$$
$$+ (k_2 k_3 + k_1 k_4) \operatorname{sh} k_2 \sin k_1] f_2^{-1},$$

$$f_{12s}^{(l)} = Q(l)|_{\phi(l)=1}$$
$$= -e_s l_s^{-2} k_3 k_4 (k_1 k_3 + k_2 k_4)(\operatorname{ch} k_2 - \cos k_1) f_2^{-1},$$

$$f_{21s}^{(0)} = M(0)|_{v(0)=1} = f_{12s}^{(0)},$$
$$f_{21s}^{(l)} = M(l)|_{v(l)=1} = f_{12s}^{(l)},$$
$$f_{13s}^{(0,l)} = f_{31s}^{(0,l)} = f_{23s}^{(0,l)} = f_{32s}^{(0,l)} = 0,$$
$$f_{22s}^{(0)} = M(0)|_{\psi(0)=1}$$
$$= e_s l_s^{-1}(k_1 k_3 + k_2 k_4)(k_4 \operatorname{ch} k_2 \sin k_1$$
$$- k_3 \operatorname{sh} k_2 \cos k_1) f_2^{-1},$$
$$f_{33s}^{(0)} = N(0)|_{w(0)=1} = E_s A_s l_s^{-1} h^{-1} k_5 \cot k_5,$$
$$f_{33s}^{(l)} = N(l)|_{w(l)=1} = E_s A_s l_s^{-1} h^{-1} k_5 \csc k_5,$$
$$f_2(k_1,k_2) = 2k_3 k_4 (\operatorname{ch} k_2 \cos k_1 - 1)$$
$$+ (k_3^2 - k_4^2) \operatorname{sh} k_2 \sin k_1,$$
$$e_s = E_s I_s h^{-1},$$
$$k_{1,2} = l_s k_B', \quad k_{3,4} = k_{2,1}\left(1 \pm \frac{k_{1,2}^2 k_{20}^2}{l_s^2(k_B^4 - k_{10}^2 k_{20}^2)}\right),$$
$$k_5 = l_s k_{10}, \quad k_B = (k_{10}^2 i^{-2})^{1/4},$$
$$k_B' = (\pm [(k_{10}^2 + k_{20}^2)/2]$$
$$+ \{[(k_{10}^2 - k_{20}^2)/2]^2 + k_B^4\}^{1/2})^{1/2}, \tag{4}$$

where k_B is the bending-type wave number, k_B' is the bending-type wave number considering shear deformation and rotational inertia, i is the radius of inertia, A_s and I_s are area and moment of inertia of the stiffener's cross section per unit length of the shell.

III. SOLUTION OF THE PROBLEM

Fourier transforms of the unknown functions are expanded in series of normal modes,

$$u_j = \sum_{m=-\infty}^{\infty} u_{jm} e^{im\theta}, \quad j = 1,2,3, \tag{5}$$

$$p_i = p_0 g(\omega) \sum_{m=-\infty}^{\infty} (-i)^m J_m(\omega r) e^{im\theta}, \tag{6}$$

$$p = p_0 g(\omega) \sum_{m=-\infty}^{\infty} (-i)^m X_m(\omega) H_m^{(1)}(\omega r) e^{im\theta}; \tag{7}$$

here, p_0 is the constant with the units of pressure, $g(\omega)$ is the spectral response function to be discussed further, J_m is the Bessel function, $H_m^{(1)}$ is the Hankel function of the first kind, and X_m is the unknown coefficient of the expansion of the scattered pressure.

Displacements of the shell at the junction lines can be written in the form

$$u_j(\theta)\delta(\theta - \theta_s) = \left(\frac{1}{2\pi}\right) u_j(\theta_s) \sum_{m=-\infty}^{\infty} e^{im(\theta - \theta_s)}. \tag{8}$$

Due to linearity, the total solution of the problem is divided into two parts: p^0, corresponding to the well-known unstif-

fened shell solution[12] and p^*, describing the contribution of the stiffening members or a stiffener-borne sound. To determine the coefficients of the expansion of the displacements and the scattered pressure field, one obtains, on the basis of Eqs. (1)–(3) two subsystems:

$$a_{ij} u_{jm}^0 = \delta_{k3} q_{rm}, \tag{9}$$

$$a_{ij} u_{jm}^* = \sum_{s=1}^{S} T_{js}[u_j(\theta_s), f_{ijs}] e^{im\theta}, \quad i,j = 1,2,3, \tag{10}$$

where a_{ij} denotes the coefficients of the theory of shells.[12] Displacements $u_j(\theta_s)$ are constants, which are to be determined from the condition of the continuity of deformations

$$u_j(\theta_s) = \sum_{m=-\infty}^{\infty} (u_{jm}^0 + u_{jm}^*) e^{im\theta_s}; \tag{11}$$

as the expression for u_{jm}^* contains the constants $u_j(\theta_s)$, one obtains a system of linear algebraic equations of order $3S$ in the unknowns $u_j(\theta_s)$. To determine the coefficients of this system one has to sum the series that may be regularized by extraction of singularities. In the special case of stiffening members lying entirely along one diameter the matrix of coefficients of the governing system of equations decomposes into two subsystems: one corresponding to the antisymmetric components (u_1,u_2), and another to the symmetric component u_3 of the displacements. Thus one can separate from pressure p^* one part p_s^* associated with symmetric shell modes (forms of vibrations) relative to the stiffener, and another associated with antisymmetric shell modes. Once the constants $u_j(\theta_s)$ have been found, the contribution of the stiffeners to the steady-state echo signal (7) is also determined. The coefficient of the expansion for the scattered pressure field is

$$X_m = X_m^0 + X_m^*, \tag{12}$$

where

$$X_m^0 = -[\omega J_m'(\omega) A_{33} - \xi J_m(\omega) D] f^{-1}(\omega),$$

$$X_m^* = -\sum_{s=1}^{S} \sum_{j=1}^{3} T_{js} A_{js} \exp\left[-im\left(\theta_s + \frac{\pi}{2}\right)\right] f^{-1}(\omega),$$

$$f(\omega) = \omega H_m^{(1)'}(\omega) A_{33} - \xi H_m^{(1)}(\omega) D.$$

Here, J_m is a Bessel function, the prime denotes a derivative of the functions with respect to argument, and A_{ij} and D are the minor and determinant of the matrix $\{a_{ij}\}$ from Eqs. (9) and (10). It must be pointed out that both parts of Eq. (12) have the same denominator, and thus no new types of waves are expected. In the framework of the Timoshenko–Mindlin theory of plates and shells only three types of waves can be observed: membrane, flexural, and shear. The sound pressure field as a function of time can be determined by inverse Fourier transformation,

$$p(r,\theta,t) = \frac{1}{2\pi} \int_{-\infty}^{\infty} p(r,\theta,\omega) e^{-i\omega t} d\omega,$$

where p is given by expression (7). The spectral response function in the case of a short Gaussian pulse,

$$p_i(r,\theta,t) = p_0 \exp(-\alpha^2 t^2 - i\omega_0 t),$$

has the form

$$g(\omega) = 1/(2\sqrt{\pi}a)e^{-[(\omega - \omega_0)/2a]^2},$$

where ω_0 is a carrier frequency.

IV. NUMERICAL RESULTS AND THEIR ANALYSIS

The calculations refer to the scattering of a plane wave of unit amplitude by an aluminum shell ($E = 70$ GPa, $v = 0.335$, and $\rho_1 = 2.7$ g/cm^3) with the relative thickness $h = 0.02$. The incident wave may be either steady state or Gaussian with duration $\Delta\tau = 1$ ($\tau = ct/R$), and the carrier frequency $\omega_0 = 60$.

A. A shell reinforced by a rigid stringer

The first part of the calculations refers to the shell reinforced by a rigid stringer with thickness $h_s = 0.02$, radial dimension $l_s = 0.07$, and density of aluminum. The angle between the direction of the incidence and the stringer is $\theta_s = 60°$.

In Fig. 2 a steady-state scattered pressure field amplitude as a function of the dimensionless frequency (form function) in the far field is presented. The observing point is at the coordinate $\theta = 0°$ (backscattering). The solid curve in Fig. 2(a) shows the form function for the reinforced shell and the dashed curve that for an unreinforced shell.

The antiresonances of the form functions occuring at the greater period in both stiffened and unstiffened shells are identified as the membrane propagation-type wave. The series of sharp resonances appearing in the reinforced shell show the flexural-type wave contribution to the scattered field, whereas in the unreinforced shell, excited in the same frequency range flexural waves does not appear, as their phase velocity is subsonic.

In Fig. 2 the stiffener-borne contributions of symmetric [Fig. 2(b)] and antisymmetric p_a^s [Fig. 2(c)] forms of vibrations relative to the stringer in the scattered field are presented. Solid curves related to the elastic stringer and dashed curves to the rigid one. In the latter case wave processes in

the stringer are disregarded and the influence of the stringer to the movements of the shell is that of the attached mass. Comparison of these form functions shows that antisymmetrical forms of vibrations are more sensitive to the changes of the elastic properties of the rib at frequencies $\omega > 5$, than symmetrical ones, where the contribution of elasticity to the form function p_s^s is negligible.

To obtain the time domain response, a frequency spectrum is determined in the frequency range whose central frequency is the carrier frequency for the time-domain pulse. Such spectra are presented in Fig. 3. Here, Fig. 3(a) has the same meaning as in the previous picture and Fig. 3(b) and (c) are contributions p_s^s and p_a^s, respectively. It must be pointed out that the presence of elasticity makes spectrum p_a^s much more complicated.

Taking the Fourier transform in the given frequency one obtains the time dependence of the investigated wave processes. Echo signals for the unreinforced shell are presented in Fig. 4(a). The pulse specularly reflected from the front surface of the shell is coming first, accompanied by the flexural-type pulses (slower ones, with greater amplitude) and membrane-type pulses (faster ones, with little amplitude, marked by arrows). Contribution p_s^s is shown in Fig. 4(b) and p_a^s in Fig. 4(c). In Fig. 4(d) the p_s^s contribution is presented where wave processes are not taken into consideration. In that case p_s^s and p_a^s are very much the same, except for a more complicated background in the latter one.

To help interpret the wave processes one can find the pressure field in the fluid at the surface of the shell. The pressure is shown in Fig. 5 for the cylindrical shell with the same parameters and reinforced by one rigid stringer. The spectra are calculated in the frequency range where strong flexural oscillations in the unreinforced shell occur. The corresponding pulse excitation is presented in Fig. 6. The echo signal scattered by the unreinforced shell is presented in Fig. 6(a), stiffeners' contributions p_s^s and p_a^s in Fig. 6(b) and (c), and the total echo signal in Fig. 6(d).
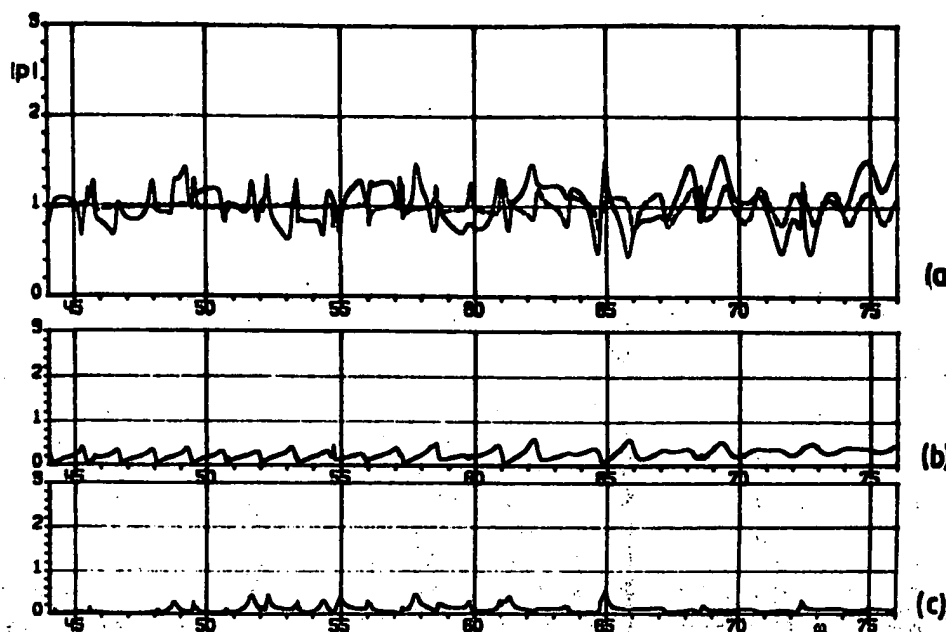

FIG. 2. Backscattered sound pressure amplitude as a function of frequency (far field). (a) Unreinforced shell (dashed line), shell reinforced by elastic stringer. $l_s = 0.07$ (solid line). (b) p_s^s contribution of elastic (solid line) and rigid stringers (dashed line), and (c) the same for the p_a^s contribution.

FIG. 3. Backscattered sound pressure amplitude as a function of frequency (far field). (a) Unreinforced shell (dashed line), shell reinforced by the elastic stringer, $l_s = 0.07$ (solid line), (b) p_r^s contribution of the elastic stringer, and (c) p_σ^s contribution of the elastic stringer.

Further analysis may be performed on the basis of decomposition of the echo signals, represented in Fig. 7, where the individual pulses are decomposed at the left side of the picture and the eikonals of the corresponding waves at the surface of the shell are shown at the right side.

Pulse 1 is that of the incident pressure pulse and pulses 2 are the flexural-type pulses, having the phase velocity approaching that of the sound velocity in the surrounding fluid. Therefore, the flexural-type pulses enter and leave the shell in the critical points $\theta = \pm \pi/2$. That type of pulses are present in the unreinforced shell together with the membrane propagation-type pulses, which are disregarded due to their smallness in the echo structures, whereas corresponding resonances in the spectra are significant. Pulses 3–5 are attributable to the presence of the stringer. All pictures are
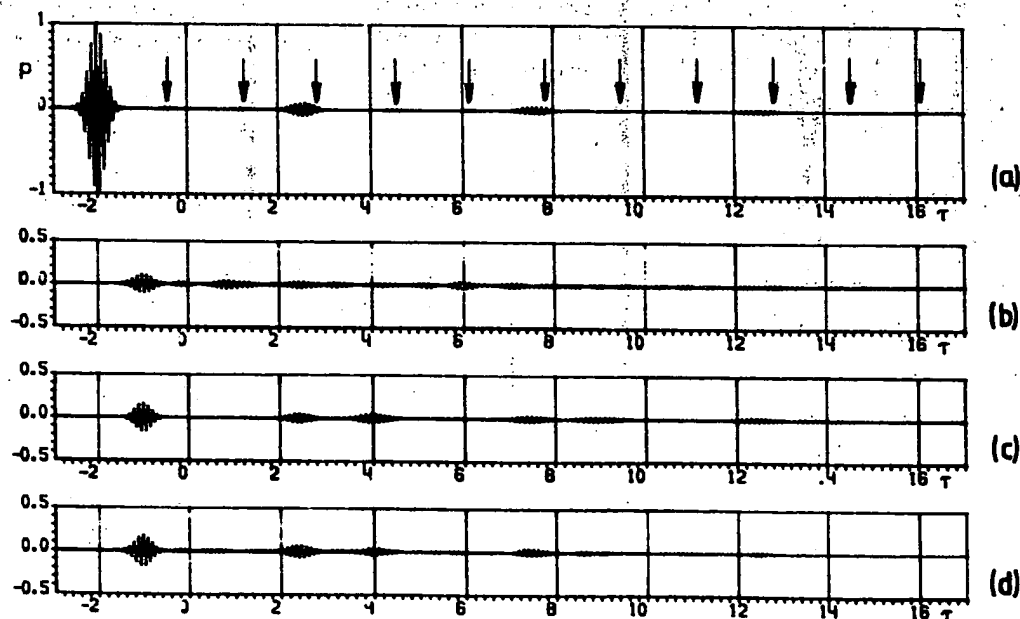

FIG. 4. Echo signal from the cylindrical shell stiffened by stringer $l_s = 0.07$ (far field). (a) Unreinforced shell, (b) p_r^s contribution of the elastic stringer, (c) p_r^s contribution for the elastic stringer, and (d) p_σ^s contribution of the same stringer, taken as rigid.
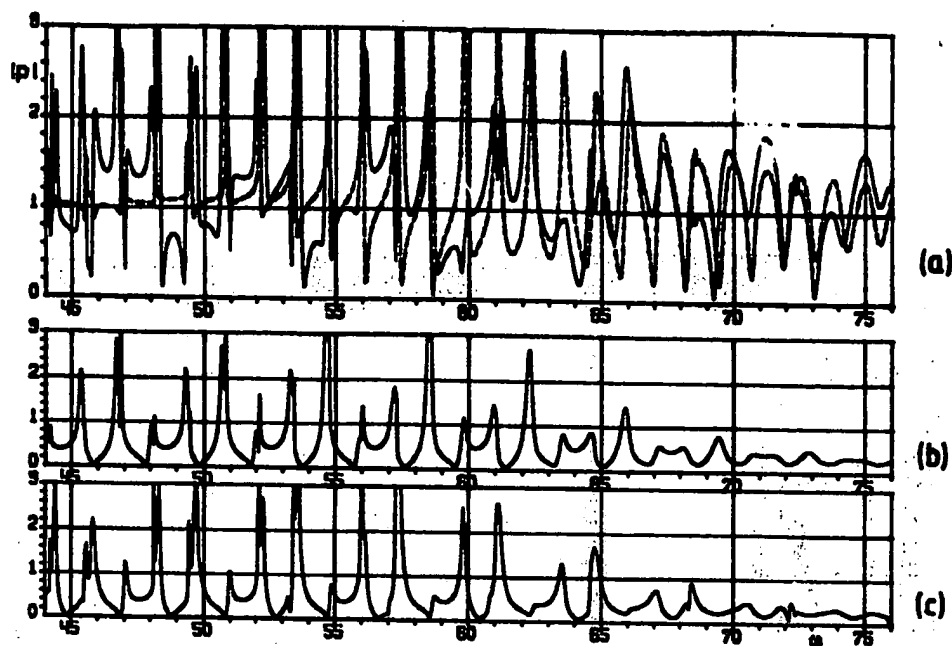
FIG. 5. Backscattered sound pressure amplitude as a function of frequency (near field). (a) Unreinforced shell (dashed line), shell reinforced by rigid stringer, $l_s = 0.07$ (solid line), (b) p_s° contribution of the stringer, and (c) p_a° contribution of the stringer.

valid for both discussed sound scattering mechanisms p_s° and p_a°.

Thus the shell/stringer junction acts as an additional entry and exit point of the circumferential waves of the flexural type.

B. A shell reinforced by an elastic stringer

Next, the influence of the elastic behavior of the stringer on sound scattering is investigated. Let us suppose the radial dimension of the stringer to be equal to the diameter of the
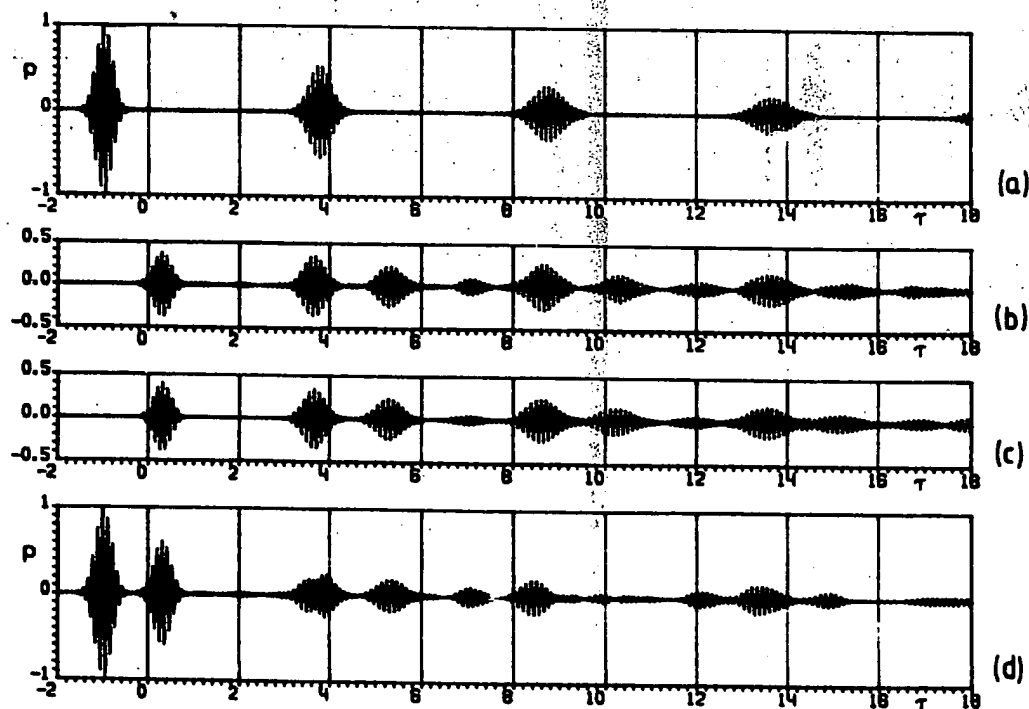
FIG. 6. Echo signal from cylindrical shell reinforced by rigid stringer $l_s = 0.07$ (near field). (a) Unreinforced shell, (b) p_a° contribution of the stringer, (c) p_s° contribution of the stringer, and the (d) reinforced shell.
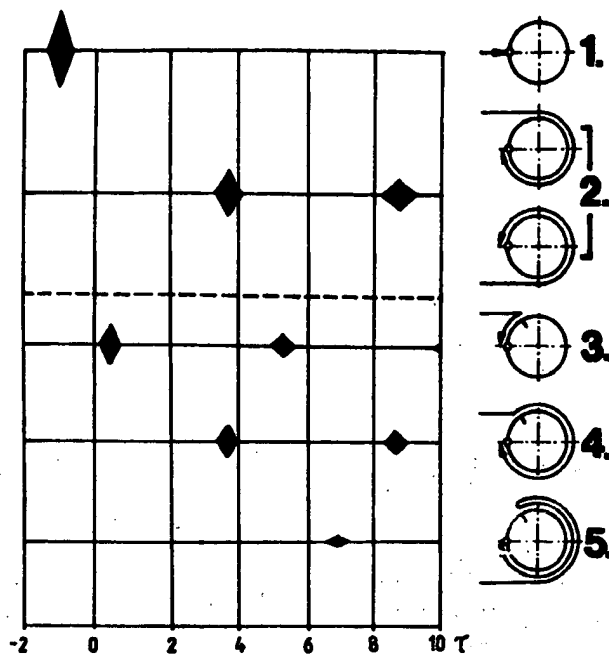
FIG. 7. Decomposition of the echo signal. (1) Specularily reflected pulse, (2) flexural-type pulses, and (3)–(5) pulses attributable to the presence of a stringer.

shell although attached to the shell at only one end. This makes it possible to see better the pulses propagating in the stringer.

Echo signals in Fig. 8 are related to the sound scattering by an aluminum shell with thickness $h = 0.02$ stiffened by an aluminum stringer at coordinate $\theta = 60°$ while the observation point is at $\theta = 0°$. The radial dimension of the stringer $l_s = 2$ and the thickness equals that of the shell. The echo contributions p_a^* and p_s^* are represented in Fig. 8(b) and (c). Decomposition of this echo signal can be seen in Fig. 9. Apart from pulses observed in the unreinforced shell (pulses 1,2), and that connected with a reflection from the stringer as a rigid body (pulses 3,6), new pulses produced by propagation and multiple reflections in the stringer appear. Vibration modes that are antisymmetric with respect to the stringer (mechanism p_a^*) produce a flexural-type pulse propagating in the stringer (pulse 4). The phase velocity of this flexural wave, according to the Timoshenko theory of plates, can be found as

$$c_B' = \omega/k_B',$$

where k_B' is the wave number defined by Eq. (4). The group velocity of the flexural wave can be determined by the expression given in Ref. 13,

$$c_{gr} = \left(\frac{dk_B'}{d\omega}\right)^{-1} = \frac{c_B'u}{u - (c_B'/c_B)^4},$$
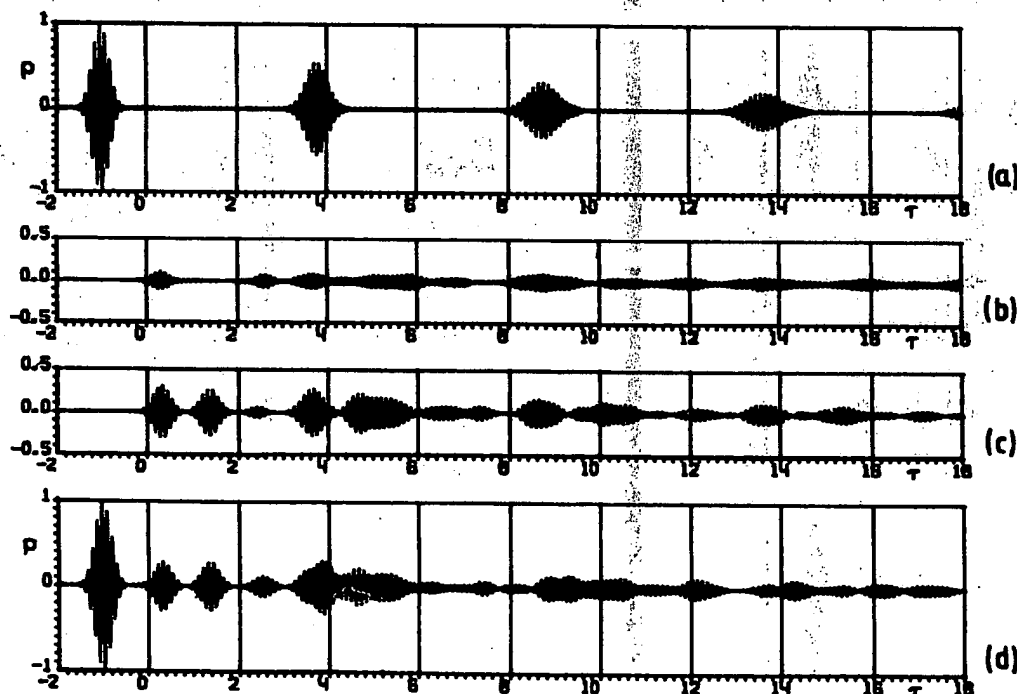

FIG. 8. The echo signal from the cylindrical shell reinforced by stringer $l_s = 2.0$ (near field). (a) Unreinforced shell, (b) p_a^* contribution of the stringer, (c) p_s^* contribution of the stringer, and (d) reinforced shell.
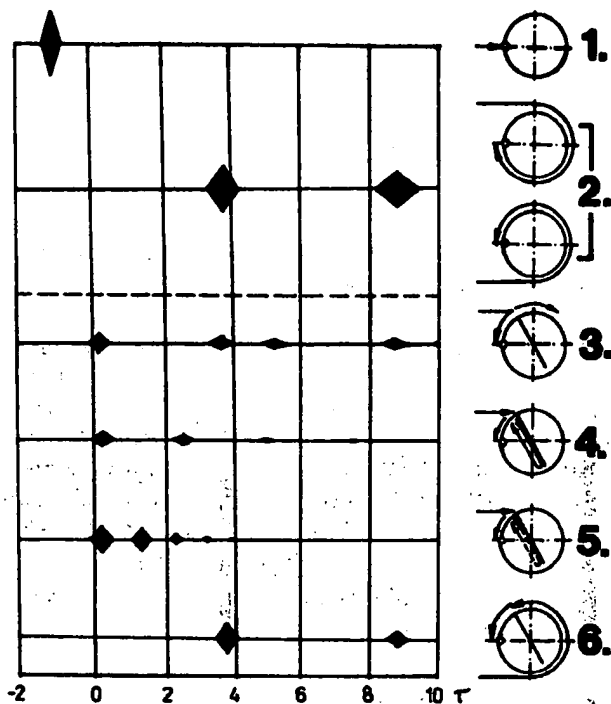
FIG. 9. Decomposition of the echo signal. (1) Specularily reflected pulse, (2) flexural-type pulses, and (3)–(6) pulses attributable to the presence of a stringer.

$$\kappa = 2 - (c_{20}^{-2} + c_{10}^{-2})(c_B')^2,$$

where c_B is velocity of the bending wave in the Kirchhoff theory. Calculations show that $c_{gr} = 2415$ m/s and $c_{gr}/c = 1.71$. Thus the flexural wave pulse propagates in the stringer about 70% faster than in the fluid-loaded shell.

Vibration modes that are symmetric with respect to the stringer (mechanism p_s^*) produce a membrane-type pulse propagating in the stringer (pulse 5 in Fig. 9). Group velocities of this pulse in the stringer and in the shell are not noticeably different. The membrane-type pulse reflected from the free edge of the stringer then retransforms itself into the flexural-type pulse propagating around the shell. As there is not radiation inside the shell, the first pulse reflected from the front edge of the stringer and that reflected from the back edge have almost the same amplitude.

C. A shell reinforced by an internal wall

The numerical results refer to the scattering of a plane sound wave by an aluminum shell with the same parameters as in Sec. IV B. The shell is reinforced by an aluminum internal wall having a thickness equal to that of the shell and attached at coordinates $\theta_s = 60°$ and $\theta_s = 240°$.

Figure 10 shows the time dependence of the sound field on the surface of the shell at the observing point $\theta = 330°$. Figure 10(a) presents the pulse structure in the unreinforced shell. Figure 10(b) and (c) represents stiffener-borne wave-generation mechanisms p_a^* and p_s^*, respectively, and Fig. 10(d) shows the total echo structure.
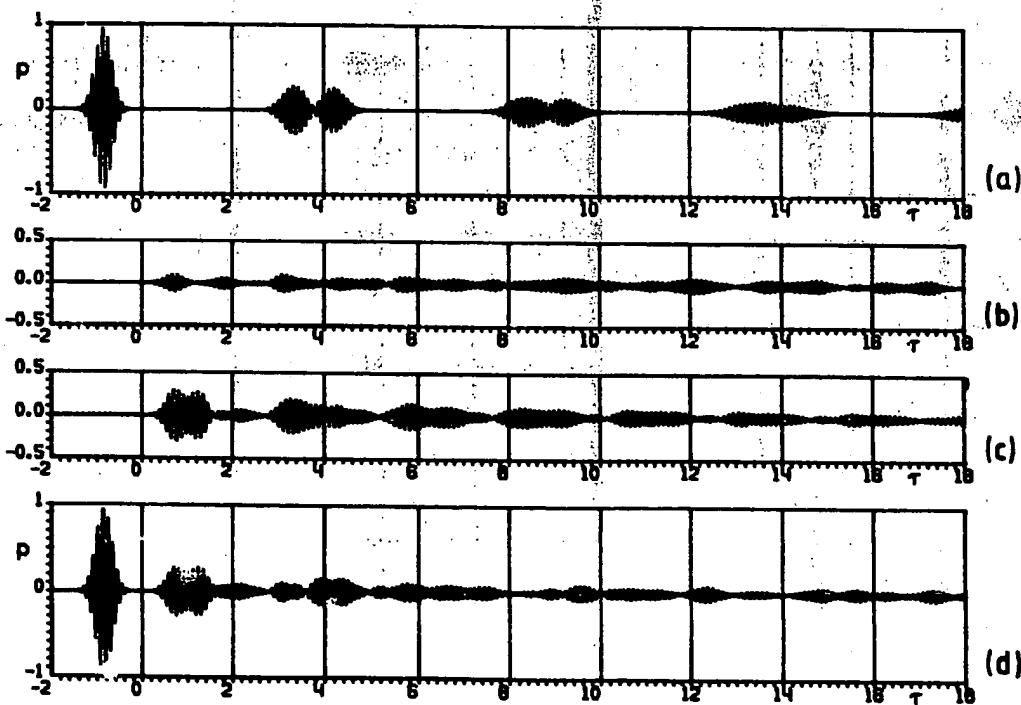

FIG. 10. Echo signal from the cylindrical shell reinforced by the internal wall, observing point at $\theta = 330°$ (near field). (a) Unreinforced shell, (b) p_a^* contribution of the wall, (c) p_s^* contribution of the wall, and (d) reinforced shell.
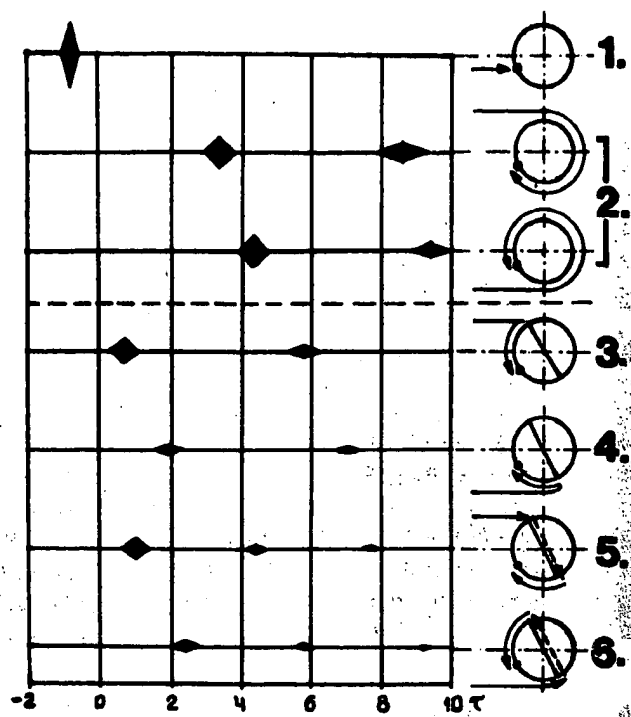
FIG. 11. Decomposition of the echo signal. (1) Specularily reflected pulse, (2) flexural-type pulses, and (3)–(6) pulses attributable to the presence of an internal wall.
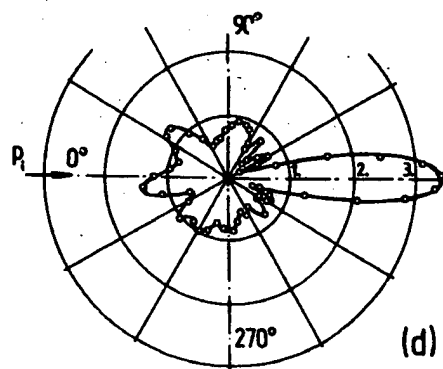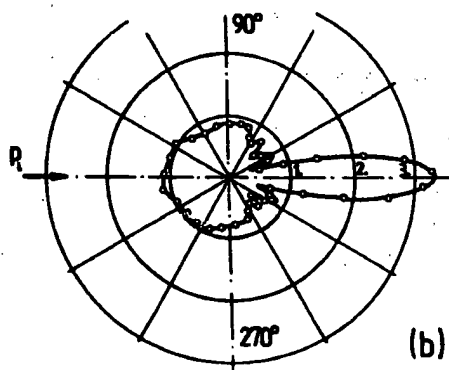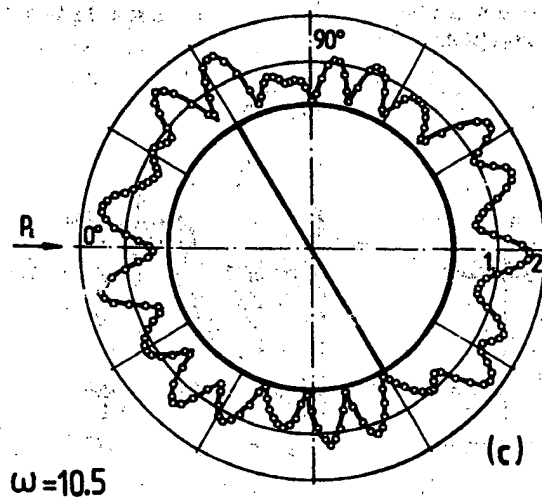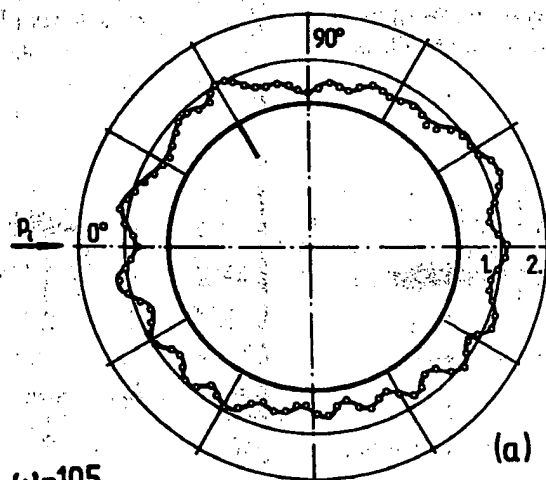

FIG. 12. Comparison of the results obtained analytically (solid line), and by the FEM and BEM (dotted line). (a) Near field and (b) far field for the shell, reinforced by the stringer, (c) near field, and (d) far field for the shell, reinforced by the wall.

The detailed analysis of individual pulses for $\theta = 330°$ can be traced in Fig. 11. In addition to wave reflections described in the previous section a new one connected with the transmission of waves through the wall appears. In the antisymmetric wave-generation mechanism p_a^e the outer reflection from the ends of the wall prevails, as in the case of the rigid stringer. In the symmetric wave-generation mechanism p_s^e in addition to the outer reflection, the flexural-type pulses (pulses 5 and 6) penetrate into the wall and propagate there transformed into membrane-type pulses. At the other end of the wall they continue their circumnavigation retransformed as flexural-type pulses. Inner reflections from the end of the wall are in the shadow zone and are about three times less than in the case of the stringer, so that most of the energy is transmitted through the wall, forming a new path for circumnavigations.

V. VERIFICATION

To verify numerical results obtained by the analytical approach presented in Sec. III, a cylindrical shell reinforced by a stringer and another one reinforced by an internal wall have been calculated by the author of Ref. 14 using numerical techniques based upon the FEM and BEM combination.

The numerical results relate to the two-dimensional (2-D) scattering problem on a steel shell stiffened by a stringer or an internal wall with a relative thickness $h = 0.05$ for both shell and stiffener. The radial dimension of the stringer $l_s = 0.25R$. The angle between the incident plane wave direction and the stiffener is $\theta = 60°$. Angular diagrams for sound pressure scattered by a shell reinforced by the stringer are presented in Fig. 12(a) for the near field and in Fig. 12(b) for the far field. Angular diagrams for the shell with the internal wall are shown in Fig. 12(c) for the near field

and in Fig. 12(d) for the far field. The solid curves represent analytical calculation and the dotted lines represent calculations obtained by the numerical method. The results are in good agreement.

VI. CONCLUSIONS

In the case of a lengthwise reinforced shell a solution can be entirely derived in closed form by the extension of the method of the separation of variables; shell/stiffener junctions act as additional entry and exit points (lines) of circumferential waves circulating in the shell and the fluid; and the junctions make possible a transformation of circumferential waves from one propagation type to another.

[1] G. Maidanik, J. Acoust. Soc. Am. 46, 1062–1073 (1969).
[2] D. G. Crighton and G. Maidanik, J. Sound Vib. 75, 437–452 (1981).
[3] I. P. Konovaljuk and V. N. Krasilnikov, "Influence of Stiffening Rib on Plane Sound Wave Reflection from a Thin Plate," in *Scattering and Radiation of Waves* (Leningrad State Univ., Leningrad, 1965), Vol. 4, pp. 149–165 (in Russian).
[4] B. P. Belinskii, Sov. Phys. Acoust. 29, 420–427 (1983).
[5] M. V. Bernblit, Sov. Phys. Acoust. 21, 518–521 (1976).
[6] M. C. Junger, J. Acoust. Soc. Am. 24, 366–373 (1952).
[7] C. B. Burroughs, J. Acoust. Soc. Am. 75, 715–722 (1984).
[8] V. N. Evseev, "Sound Radiation by a Shell with Lengthwise Stiffening Ribs", Akust. Zh. 35, 1072–1078 (1989) (in Russian).
[9] A. Klauson and J. Metsaveer, Sov. Phys. Acoust. 35, 42–47 (1989).
[10] I. Mirsky and G. Herrmann, J. Acoust. Soc. Am. 29, 1116–1123 (1957).
[11] V. Kolousek, *Dynamics of Civil Constructions* (Stroiizdat, Moscow, 1965), pp. 119–126 (in Russian).
[12] J. A. Metsaveer, N. D. Veksler, and A. S. Stulov, *Diffraction of Acoustic Pulses by Elastic Bodies* (Nauka, Moscow, 1979), pp. 167–174 (in Russian).
[13] Y. L. Shenderov, *Sound Radiation and Scattering* (Sudostroyenie, Leningrad, 1989), pp. 250–258 (in Russian).
[14] U. Ross and A. Lahe, "Radiation of Acoustic Waves by Noncircular Cylindrical Shell in Fluid," Proc. Estonian Acad. Sci. Phys. Math. 39, 40–45 (1990) (in Russian).